Effect of London Forces upon the Rate of Deposition of Brownian Particles

Rates of deposition of particles onto a spherical collector, immersed in a creeping fluid, are calculated as a function of Peclet number, aspect ratio, and the ratio of Hamaker's constant to kT for all cases of practical importance involving convective-diffusion and London forces. Boundaries of regions where London forces or Brownian motion may be neglected are established in terms of the above dimensionless groups. Gravitational forces were included in the calculations for some representative conditions but may be neglected for small or neutrally buoyant particles or for high flow rates.

Close agreement was noted between deposition rates calculated by summing individual contributions from each transport mechanism and deposition rates calculated from a rigorous consideration of their combined effect. Thus the additivity rule was verified for the cases studied.

DENNIS C. PRIEVE

Department of Chemical Engineering
University of Delaware
Newark, Delaware 19711

and

ELI RUCKENSTEIN

Faculty of Engineering and Applied Science
State University of New York at Buffalo
Buffalo, New York 14214

SCOPE

Deep-bed granular filters are used to clarify fluids containing a small amount of fine particulate matter. Spaces between grains of the bed are generally quite large compared with the size of the suspended particles so that the bed does not act like a sieve. Instead the bed provides a surface on which the particles may stick by the action of London (van der Waals) forces. Besides holding the particles to the collector surface, London forces may act over a sufficiently long range to aid in the transport of particles to the surface.

The effectiveness of deep-bed filters in removing suspended particles is measured by the value of the filter coefficient which in turn is related to the capture efficiency of a single characteristic grain of the bed. Capture efficiencies are evaluated in the present paper for all cases of practical importance in which London forces and convective-diffusion serve to transport particles to the surface of a spherical collector immersed in a creeping flow field. Gravitational forces are considered in some cases, but the general results apply mainly to submicron or neutrally buoyant particles suspended in a viscous fluid such as water. Results obtained by linearly superimposing the individual contribution from each mechanism are compared with those obtained from a rigorous coupling of mechanisms in order to test the additivity rule.

Suspended particles are considered to have finite size; thus both the mobility coefficient and diffusion coefficient of the particles depend not only on the size of the particle but also upon the distance between the particle and the collector. A numerical finite-difference technique is used to solve the general transport equation.

Several limiting cases are discussed in order to obtain insight and perspective. To identify these limiting cases, some quantity is sought for each mechanism which will characterize its relative importance.

The objectives of the present paper are to: (1) compute the rate of deposition of particles onto a spherical collector in a creeping flow field for all situations in which London forces and convective-diffusion act as transport mechanisms, (2) identify limiting behaviors according to the relative values of the characteristic parameters for each mechanism, (3) establish the physical conditions in which each of the limiting cases is valid, and (4) test the accuracy of the additivity rule.

CONCLUSIONS AND SIGNIFICANCE

The capture efficiency or Sherwood number was shown to be a function of three dimensionless groups—the Peclet number, the aspect ratio (collector radius divided by particle radius), and the ratio of Hamaker's constant (indicating the intensity of London forces) to the thermal energy of the particles. Calculated values for the rate of deposition, expressed as the Sherwood number, are plotted in Figure 6 as a function of the three dimensionless groups.

The distance from the collector surface over which each mechanism or effect exerts an influence was found to be a useful characteristic parameter. Table 1 lists the five lengths used to identify each of the limiting cases summarized by Table 2. Three principal limiting cases were considered: (1) situations where London forces are negligible, (2) situations in which diffusion is negligible, and (3) situations where the fluid motion is negligible. Several subcases appear for various orderings of other lengths. Regions of applicability for each of the limiting cases, along with the corresponding rate, are outlined in Table 3.

For those cases in which gravitational forces are also included, values of the Sherwood number are summarized in Figure 8. The ratio G of the gravitational potential of a particle, located one particle radius above the collector, to the thermal energy was used to characterize the effect of gravity. For an aspect ratio of 100, gravitational forces were found to be negligible when $G < 10^{-2}$.

Superimposing the individual contribution of each mechanism was found, in those cases tested, to yield very nearly the same overall deposition rate as obtained by rigorous consideration of coupling.

Correspondence concerning this paper should be addressed to E. Ruckenstein. D. C. Prieve is with the Department of Chemical Engineering, Carnegie-Mellon University, Pittsburgh, Pennsylvania 15213.

Because colloidal particles have finite size, their mobility and diffusion coefficients depend not only upon their size but also upon the distance from the collector surface. This variation with distance stems from friction between the collector surface and the fluid which increases the force required to push the fluid out of the path of the approaching particle. In the usual transport equation containing only convective and diffusive terms, the size of the molecules is small enough for the thickness δ_m to be small compared to the length δ_D, where δ_m and δ_D are explained in Table 1. Other situations arise in which these conditions are not met, or in which London or gravitational forces are important. To identify the limiting cases, it is useful to seek some quantity for each mechanism which allows the ordering of its relative importance.

For the case of purely attractive forces (such as London-van der Waals forces) the length δ_F over which they act is a useful characteristic. An attractive force which acts over a distance which is much less than δ_D will not contribute substantially to the overall rate. When repulsive forces (such as the electrostatic double-layer forces) are also present, they may effectively prevent particles from arriving at the collector, even when they act only over a very short distance. For this reason the decay length alone cannot characterize the relative importance of the joint effect of attractive and repulsive forces. Useful characteristics of their combined effect may be obtained by considering the total potential energy of interaction between the particle and the collector.

When repulsive forces are acting together with attractive forces, the parameter which best characterizes the effect of the repulsive force is the height E of the energy barrier defined in Figure 1. If E is large enough, the particles at $h_{\min}$ will experience difficulty in overcoming the barrier. Should the thickness of the region in which London and double-layer forces contribute substantially to the flux also be small compared to δ_D, then the effect of the interaction forces can be lumped into a boundary condition of the transport equation which takes the form of an apparent, first-order, chemical reaction (Ruckenstein and Prieve, 1973; Spielman and Friedlander, 1974). On the other hand, should the barrier be small enough, the repulsive forces will have little effect.

The present paper deals with suspensions in nonpolar solvents or in aqueous solutions of moderate or high ionic strength, where double layer forces are negligible. Gravitational forces are considered in a number of representative cases; however, the emphasis is upon the mechanisms of convective-diffusion and London forces. Several limiting cases occur which can be classified by an ordering of the characteristic lengths summarized by Table 1. Three principal limiting behaviors may be identified: (1) situations where London forces are negligible, (2) situations where diffusion is negligible, and (3) situations where fluid motion is negligible. Table 2 identifies each case and lists the corresponding investigator and technique employed. Several subcases appear due to various orderings of the other lengths.

THEORETICAL DEVELOPMENT AND SOLUTION OF TRANSPORT EQUATION

When an isolated sphere is held stationary in a creeping flow field containing suspended particles (see Figure 2), the equation of continuity in spherical coordinates, allowing azimuthal symmetry, is given by

$$\frac{1}{r^2}\frac{\partial}{\partial r}(r^2 N_r) + \frac{1}{r\sin\theta}\frac{\partial}{\partial\theta}(N_\theta \sin\theta) = 0 \qquad (1)$$

TABLE 1. CHARACTERISTIC LENGTHS

Length	Definition
δ_F	Length over which London forces contribute substantially to the radial particle flux.
δ_D	Length over which convective-diffusion contributes substantially to the radial particle flux.
δ_m	Length over which the mobility and diffusion coefficients vary appreciably with radial distance.
a	Collector radius.
a_p	Particle radius.

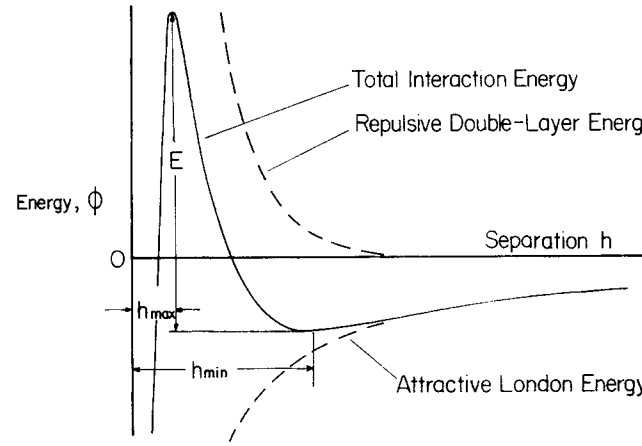

Fig. 1. Profile of the total energy of interaction between a colloidal particle and the collector surface arising from the double-layer repulsion and London attraction.

The radial and tangential components of the total particle flux vector, taken to be positive in the direction of increasing r or increasing θ, can be written as

$$N_r = v_r c - D\frac{\partial c}{\partial r}, \text{ and} \qquad (2a)$$

$$N_\theta = v_\theta c, \qquad (2b)$$

where the first term (proportional to c) represents the particle flux resulting from London forces and fluid motion; thus v_r and v_θ may be interpreted as the non-Brownian particle velocities. Except far from the collector, these are not equivalent to the corresponding components of the fluid velocity since particle trajectories do not coincide with fluid streamlines even in the absence of Brownian motion or interaction forces.

Non-Brownian Particle Velocities

By performing a radial force balance, Spielman and Fitzpatrick (1973) determined the radial velocity of a particle attracted to a spherical collector by London forces when particle inertia and Brownian motion are negligible:

$$\underbrace{\frac{v_r(h,\theta)}{m(h/a_p)}}_{\text{viscous drag}} = \underbrace{\frac{s_r(h,\theta)\, f_2(h/a_p)}{m_*}}_{\text{fluid motion force}} - \underbrace{\frac{2}{3}\frac{Aa_p^3}{(h+2a_p)^2 h^2}}_{\text{London force}} \qquad (3)$$

Hamaker's (1937) expression for the unretarded London force was employed, whereas the expression for the force exerted by fluid motion was taken from the results of

TABLE 2. SUMMARY OF LIMITING CASES

Case	Subcase	Ordering of lengths	References	Comments
1		a_p and $\delta_F << \delta_D$		Negligible interaction forces. Continuum mechanics apply.
	a	$a_p, \delta_F, \delta_m << \delta_D << a$	Levich (1962) Lighthill (1950)	Diffusion boundary-layer approximation is valid. D is independent of position. Analytical solution possible.
	b	$a_p, \delta_F, \delta_m << \delta_D \sim a$	Yuge (1956)	D is independent of position. Transition between subcases *a* and *c*.
	c	$a_p, \delta_F, \delta_m, a << \delta_D$		Fluid considered stagnant. D is independent of position. Analytical solution possible.
	d	δ_F and $a_p << \delta_D$ and a	This paper	D depends on distance from surface. Numerical solution for rate.
2		$\delta_D << \delta_F$		Diffusion is negligible.
	a	$\delta_D << \delta_F << a$	Spielman and FitzPatrick (1973)	Trajectory analysis used. Approximate velocity profile, only valid near collector, is used.
	b	δ_D and $\delta_F << a_p$	Fuchs (1964)	Particle trajectories assumed to coincide with fluid streamlines. Capture by Interception. Analytic solution possible.
	c	$\delta_D << \delta_F$ and a	This paper	Exact fluid velocity profile used.
3		a_p and $a << \delta_D$	This paper	Fluid considered stagnant. Analytic solution possible.

Goren and O'Neill (1971), who calculated the normal force exerted by creeping flow over a sphere near a plane surface. Although the flow field in the present problem is somewhat more complex than that considered by Goren and O'Neill, the curvature of the plane surface as well as a tangential velocity component have only secondary effects upon the normal force, so their result is reasonably applicable here.

Since tangential diffusion has been neglected, only fluid motion contributes to the tangential particle velocity. Near to the collector the fluid appears to be experiencing uniform, linear, shear flow. Goldman et al. (1967b) studied the viscous motion of a sphere in Couette flow and found the particle velocity to be proportional to, but less than, the undisturbed fluid velocity at the particle's center:

$$v_\theta(h, \theta) = s_\theta(h, \theta)\, f_3(h/a_p) \tag{4}$$

In situations where separations comparable to the collector radius ($h \gtrsim a$) need to be considered, the particle no longer experiences Couette flow. However, Equation (4) correctly predicts that v_θ approaches s_θ at large separations, whereas at small separations, where the distinction between v_θ and s_θ is most important, the conditions of its derivation are practically satisfied.

Particle inertia has been assumed to be substantially smaller than the viscous drag force. This assumption will be valid provided the Reynolds number $\rho_p a_p \beta U/\mu$ is sufficiently small, which is more likely to be the case with liquids than gases.

Position-Dependent Mobility and Diffusion Coefficient

Suppose a spherical particle is moving under the action of a constant force toward a solid surface having a radius of curvature much larger than the particle. Friction between the fluid and the particle creates a drag force which opposes motion. As the particle approaches the plane solid surface, its velocity decreases as a result of an increase in the drag caused by additional friction between the fluid and the wall. This decrease in particle velocity under a constant applied force implies a decrease in particle mobility (velocity per unit applied force). When the particle Reynolds number is small, the mobility can be calculated using a modified form of Stokes's equation:

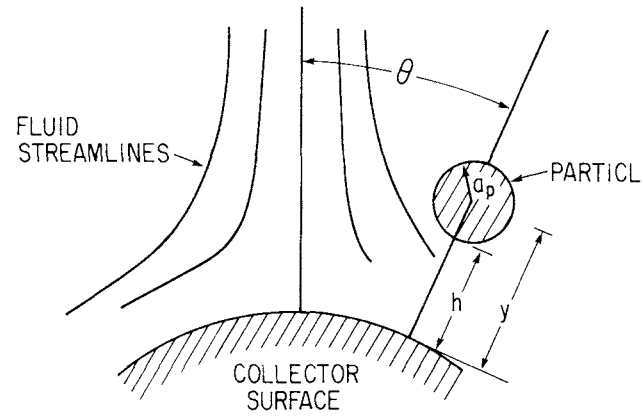

Fig. 2. Colloidal particle suspended in a fluid creeping over the surface of a spherical collector.

$$m = \frac{f_1\,(h/a_p)}{6\pi\mu a_p} \tag{5}$$

where the factor f_1 was calculated by Brenner (1961) to correct for the wall effect by considering the motion of a sphere through a quiescent fluid near a plane surface. At small separations ($h < a_p$) where f_1 becomes substantially less than unity, the fluid may be considered essentially quiescent.

According to the Nernst-Einstein equation ($D = mkT$) the mobility and diffusion coefficients are proportional. Then, using Equation (5), the diffusion coefficient of the particles can be expressed as

$$D = D_\infty f_1\,(h/a_p) \tag{6a}$$

where

$$D_\infty = kT/6\pi\mu a_p \tag{6b}$$

Brenner's correction factor $f_1(H)$ tends to H when $H << 1$ and to $(H - 1/8)/(H + 1)$ when $H >> 1$.

Undisturbed Fluid Velocities

When the flow over the collector is sufficiently slow ($\rho a\beta U/\mu < 1$), Stokes's expressions for the undisturbed fluid velocity can be used:

$$s_r = -\beta U\left[1 - \frac{3}{2}\left(\frac{a}{r}\right) + \frac{1}{2}\left(\frac{a}{r}\right)^3\right]\cos\theta \tag{7a}$$

and

$$s_\theta = \beta U\left[1 - \frac{3}{4}\left(\frac{a}{r}\right) - \frac{1}{4}\left(\frac{a}{r}\right)^3\right]\sin\theta \tag{7b}$$

For an isolated sphere β is unity and U is the approach velocity; for creeping flow around one grain of a packed bed, β is a semiempirical factor introduced to account for the effects of the bed porosity and U is the superficial velocity. Happel's (1958) model may be used (Spielman and Fitzpatrick, 1973) to estimate β. However, Happel's model assumes that flow occurs only in a narrow annulus near the surface of the grain; integration of the transport equation sometimes involves a larger region. A more adequate model does not presently exist.

Transport Equation and Its Boundary Conditions

Combining the continuity equation and flux expressions together with particle and fluid velocities, then writing the result in terms of dimensionless variables, yields the transport equation:

$$\frac{2R}{Pe}f_1(H)\frac{\partial^2 C}{\partial H^2} + \left[\frac{2R}{Pe}\left(\frac{df_1}{dH} + \frac{2f_1}{R+Y}\right) - v\right]\frac{\partial C}{\partial H} - \left[\frac{2}{R+Y}\left(v + \frac{\partial u}{\partial\theta}\right) + \frac{\partial v}{\partial H}\right]C = \frac{u}{R+Y}\frac{\partial C}{\partial\theta} \tag{8}$$

with

$$u = \left[\frac{3}{2}R^2 + Y\left(\frac{9}{4}R + Y\right)\right]\frac{Yf_3(H)\sin\theta}{(R+Y)^3} \tag{9a}$$

and

$$v = -Y^2\left(\frac{3}{2}R + Y\right)\frac{f_1(H)\,f_2(H)\cos\theta}{(R+Y)^3} - \frac{4}{3}\left(\frac{A}{kT}\right)\left(\frac{R}{Pe}\right)\frac{f_1(H)}{(Y^2-1)^2} \tag{9b}$$

Mobility and diffusion coefficients were evaluated from Equations (5) and (6). The associated boundary conditions are

$$C(H = 0, \theta) = 0, \tag{10a}$$

$$C(H = \infty, \theta) = 1, \tag{10b}$$

and

$$\left.\frac{\partial C}{\partial\theta}\right|_{\theta=0} = 0 \tag{10c}$$

The concentration of particles in contact with the collector is taken to be zero because these particles are no longer part of the disperse phase. At large distances from the collector the particle concentration must tend to that of the approaching fluid. The third boundary condition arises from the symmetry about the forward stagnation path ($\theta = 0$).

Numerical Solution of Transport Equation

The infinite radial domain ($0 \leq H < \infty$) was compressed into a finite domain ($0 \leq \eta \leq 1$) by use of the following transformation:

$$H = b\ln(1 - \eta) \tag{11a}$$

which is similar to a transformation employed by Vrentas et al. (1966). With condition (10c), the transport equation along $\theta = 0$ is an ordinary boundary value problem, for which finite differences with a uniform η-step could yield a solution. For $\theta > 0$ the technique of Crank and Nicolson (1947) was used.

When the Peclet number equals about R^3, or when $Ad < 1$ and Brownian motion is negligible, the radial concentration profile displays a maximum value greater than unity. Then a generalized form of transformation (11a)

$$H = b_1\ln(1 - \eta) + b_2\ln(1 - \eta^n) \tag{11b}$$

gave additional flexibility to distribute grid points of the H-domain both inside and outside the point corresponding to the maximum concentration.

Evaluation of the Deposition Rate

Once the concentration profile is determined that satisfies the transport equation, the radial flux can be evaluated from Equation (2a) and integrated over the collector surface to obtain the overall rate of deposition. When particles come in contact with the collector, the diffusion coefficient vanishes, leaving the radial particle flux equal to $v_r c$; however, the product $v_r c$ is indeterminant at $r = a$ ($H = 0$), since the particle concentration must vanish [Equation (10a)], while London forces are accelerating the particles to nearly infinite velocity at the moment of contact. One means of avoiding this indeterminancy is to integrate the flux over some surface other than $r = a$. From the Gauss Divergence Theorem and the continuity equation, the integral of the radial particle flux over any spherical surface concentric with the collector will have the same value regardless of the radius of the surface. Thus the following expression for the overall rate will be independent of r:

$$I = 2\pi r^2\int_0^\pi -N_r(r, \theta)\sin\theta\, d\theta \tag{12}$$

In addition to avoiding the indeterminancy at $r = a$, the observation that this expression is independent of r provides a test of the accuracy of the numerical technique used to evaluate C.

Two dimensionless forms of the rate are useful. The ratio of the actual deposition rate to the rate of convection at large distances upstream from the collector is defined as the capture efficiency:

$$e = \frac{I}{\pi a^2\beta U c_\infty} = 2\left(1 + \frac{Y}{R}\right)^2\int_0^\pi\left(\frac{2R}{Pe}f_1\frac{\partial C}{\partial H} - vC\right)\sin\theta\, d\theta \tag{13a}$$

The Sherwood number may be interpreted as twice the ratio of the actual rate to the rate computed when only diffusion is considered:

$$Sh = \frac{2I}{4\pi a D_\infty c_\infty} = \frac{1}{2}\left(1 + \frac{Y}{R}\right)^2\int_0^\pi\left[2Rf_1\frac{\partial C}{\partial H} - (Pe)vC\right]\sin\theta\, d\theta \tag{13b}$$

Eliminating I between these two equations results in the following relation:

$$Sh = \frac{1}{4}e\,(Pe) \tag{14}$$

DIMENSIONAL ANALYSIS

Inspection of the dimensionless transport equation developed above reveals that three dimensionless groups—Pe, R, and A/kT—influence the dimensionless concentration profile. Since the expressions for the capture efficiency and Sherwood number involve no additional groups, it is possible to write

$$e = e\left(Pe, R, \frac{A}{kT}\right), \quad \text{or} \tag{15a}$$

$$Sh = Sh\left(Pe, R, \frac{A}{kT}\right) \tag{15b}$$

However, for large Peclet numbers and small Hamaker's constants, the quantity eR^2 can be expressed as a function of only two dimensionless groups.

For large Peclet numbers and small Hamaker's constants, appreciable concentration variation occurs only very near to the collector. Then Stokes's expressions for the fluid velocity may be expanded in a Taylor series about the collector surface and higher order terms together with curvature effects may be neglected, yielding

$$2\frac{R^3}{Pe} f_1 \frac{\partial^2 C}{\partial H^2} + \left(2\frac{R^3}{Pe}\frac{df_1}{dH} - R^2 v\right)\frac{\partial C}{\partial H} - \left[\frac{\partial(Ru)}{\partial\theta} + \frac{\partial(R^2 v)}{\partial H}\right] C = Ru\frac{\partial C}{\partial\theta} \tag{16}$$

with

$$Ru = \frac{3}{2} Y f_3(H) \sin\theta \tag{17a}$$

and

$$R^2 v = -\frac{3}{2} Y^2 f_1(H) f_2(H) \cos\theta - \frac{4}{3}\left(\frac{A}{kT}\right)\left(\frac{R^3}{Pe}\right)\frac{f_1(H)}{(Y^2-1)^2} \tag{17b}$$

These equations involve only two independent dimensionless groups: Pe/R^3 and $\frac{4}{3}\left(\frac{A}{kT}\right)\left(\frac{R^3}{Pe}\right)$. In later discussions it will be convenient to give this second group a new name: Ad. Recalling Equation (12) for the capture efficiency, together with those immediately above, we can deduce

$$eR^2 = f(Ad, Pe/R^3) \tag{18}$$

whenever the concentration variations occur only very near to the collector surface.

RESULTS AND DISCUSSION

In the presentation of results, the principal limiting cases summarized in Table 2 will be discussed first. Then the general results will be presented, followed by the identification of the regions in which the rate predictions for each limiting case are valid. Finally, gravitational effects and the additivity rule are discussed.

Case 1: Brownian Particles with Weak London Forces

In this case London forces cause adhesion of the particles coming in contact with the collector but do not aid in the transport; hence A/kT is taken as zero. Because one of the subcases (Case 1c) is pure diffusion, it seems more reasonable to express the rate of deposition as the Sherwood number.

Figure 3 summarizes the results obtained when the contribution of London forces to the transport rate is negligible. When the boundary-layer analysis of Levich and Lighthill is valid (Case 1a) the Sherwood number is given by

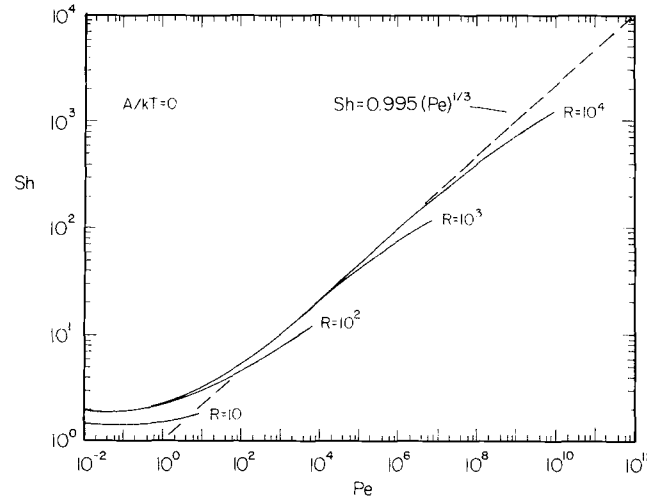

Fig. 3. Case 1. Sherwood numbers computed for the convective-diffusion of particles of finite size to the surface of a spherical collector by neglecting interaction forces. The dashed line is the Levich-Lighthill equation (19) which is valid when a diffusion boundary-layer exists and the particles are infinitesimal.

$$Sh = 0.995(Pe)^{1/3} \tag{19}$$

whereas when pure diffusion occurs (Case 1c), the Sherwood number is, by definition, two. Deviations from the Levich-Lighthill equation occur when (1) δ_D is not small compared to the collector radius, or (2) when the particle size becomes large when compared with the diffusion boundary-layer thickness. To avoid condition (1) the Peclet number must be larger than 100, whereas to avoid condition (2) the Peclet number must be smaller than $10^{-4}R^3$. The form of this latter condition may be derived by taking $\delta_m = \alpha_1 a_p$, as suggested by Equation (6), and by taking $\delta_D = \alpha_2 a(Pe)^{-1/3}$. Then $\delta_m << \delta_D$ whenever $Pe^{1/3} << \frac{\alpha_2}{\alpha_1} R$. The ratio α_2/α_1 as well as the validity of this condition can be deduced by inspection of Figure 3. Thus Equation (19) is valid in the interval $100 \leq Pe \leq 10^{-4}R^3$ when A/kT is sufficiently small.

Use of Fick's law to describe the diffusion process requires the solute particle to be small compared with the diffusion boundary layer. The analysis presented above suggests that, for Peclet numbers greater than 100, the ratio δ_D/a_p is proportional to $(Pe)^{1/3}/R$. The solid curves in Figure 3 are truncated at the value of the Peclet number corresponding to $Pe/R^3 = 10^{-2}$, where an inspection of the radial concentration profile revealed that the ratio δ_D/a_p is about ten.

Case 2: Non-Brownian Particles

All particles, regardless of their size, undergo some degree of random or Brownian motion. However, the significance of this movement as a transport mechanism is less for large particles. In this paper *non-Brownian* refers to situations in which Brownian motion may be ignored when computing particle transport rates. Neglecting the diffusive terms in the transport Equation (8), a dimensional analysis shows that the product eR^2 depends only upon R and $\frac{4}{3}\left(\frac{A}{kT}\right)\frac{R^3}{Pe}$.

The group $\frac{4}{3}\left(\frac{A}{kT}\right)\frac{R^3}{Pe}$, denoted by Ad, can also be written as

$$Ad = \frac{4}{3}\left(\frac{A}{kT}\right)\frac{R^3}{Pe} = \frac{Aa^2}{9\pi\mu a_p^4 \beta U} \tag{20}$$

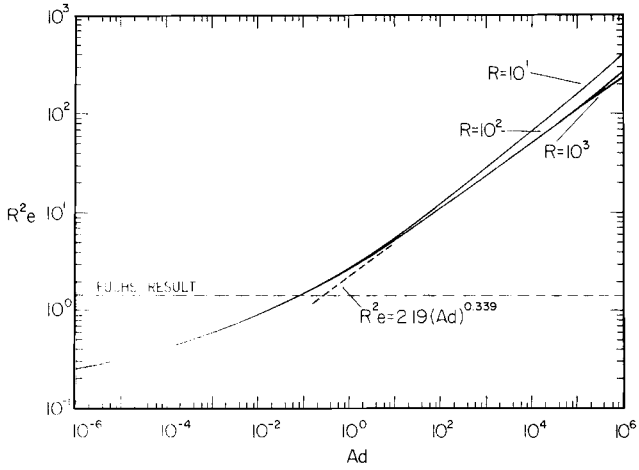

Fig. 4. Case 2. Single-grain capture efficiencies for the collection of non-Brownian particles by a spherical grain of a packed bed. A linear asymptote is noted by the dashed line which is valid for $10 < Ad < 10^{-6}R^7$.

This dimensionless group, introduced for conciseness in rate correlations, has no simple physical interpretation. It is the product of several ratios: A/kT represents the ratio of the characteristic London interaction energy to the thermal energy of the particle, R is the aspect ratio, while the Peclet number may be considered as the ratio of a characteristic energy for drag losses to the thermal energy possessed by the particle. This interpretation for the Peclet number becomes evident by using the relation $D = mkT$ to write

$$Pe = \frac{2a\beta U}{D_\infty} = \frac{2a\beta U/m_x}{kT} \tag{21}$$

Capture efficiencies are presented in Figure 4 for cases in which Brownian motion may be neglected. Small Ad implies weak London forces, hence $\delta_F << a$. From Equation (18) one then expects that eR^2 will depend only upon Ad for small Ad, as may be observed in Figure 4. Spielman and Fitzpatrick (1973) used a trajectory analysis to treat this limiting case.

Curves corresponding to large aspect ratios have a linear asymptote for large values of Ad:

$$eR^2 = 2.19\ (Ad)^{0.339}, \quad \text{for} \quad 10 < Ad < 10^{-6}R^7 \tag{22}$$

No linear asymptote is observable for small Ad. For $Ad \leq 10^{-6}R^7$ the value of eR^2 was observed to be independent of R and $\delta_F << a$.

Fuchs (1964) computed the efficiency of capture by assuming the particles always follow fluid streamlines (Case 2b). Capture takes place when a streamline approaches one particle radius of the collector surface. Fuchs's analysis yields $eR^2 = 3/2$, which is plotted in Figure 4 as the dotted horizontal line. This result does not consider the effect of Brownian motion or London forces and therefore should yield the limiting value of eR^2 for non-Brownian particles when Ad approaches zero. However, Figure 4 shows that as Ad becomes small, eR^2 computed from a more rigorous analysis is considerably smaller than 3/2. Careful analysis of particle motion in flow fields near to a solid surface have shown that the particle velocity differs considerably from the undisturbed fluid velocity at the particle's center (Goren and O'Neill, 1971; Goldman et al., 1967). The radial component of the particle velocity, deduced from Equation (3), approaches zero as the particle approaches the surface in the absence of London forces, whereas the undisturbed radial fluid velocity at the particles center does not vanish even when the particle is in contact with the surface. Particle velocities coincide with fluid velocities only when the particle is several diameters away from a solid surface. For this reason Fuchs's analysis may yield only a qualitative indication of the efficiency. It does, for example, correctly and simply show that the efficiency for non-Brownian particles and weak London forces is proportional to R^{-2}.

Case 3: Stagnant Fluid

When the velocity at which the fluid approaches the collector becomes sufficiently slow the fluid may be considered to be essentially stagnant. The continuity equation for this situation takes on a particularly simple form which can be integrated to yield

$$N_r = -\frac{\alpha}{r^2} \tag{23}$$

If the London force is expressed as the gradient of the potential energy of interaction ϕ, the total flux may be written as the sum of the London and diffusive fluxes:

$$N_r = -m\frac{d\phi}{dr}c - D\frac{\partial c}{\partial r} \tag{24}$$

Equating these two equations for the radial flux yields a first-order ordinary differential equation in c, which may be integrated to yield

$$c(\infty) - c(a + a_p) = \alpha \exp[-\phi(a + a_p)/kT] \int_{a+a_p}^{\infty} \exp[\phi(r)/kT] \frac{dr}{r^2 D(r)} \tag{25}$$

Applying the boundary conditions of Equation (10), α may be evaluated. The rate of deposition per unit area may then be calculated as $-N_r|_{r=a+a_p}$ from Equation (23). In terms of dimensionless variables the result is

$$Sh = \frac{2}{R}\left\{\int_0^{\infty} \frac{\exp(\phi/kT)}{(R + H + 1)^2 f_1(H)}\, dH\right\}^{-1}, \tag{26}$$

which is plotted in Figure 5. Small A/kT and large R correspond to pure diffusion of a solute of infinitesimal dimensions through a stagnant fluid (Case 1c) for which a_p, δ_F, δ_m and a are much less than δ_D, and the Sherwood number takes on a value of two. Both δ_m and δ_F are proportional to a_p, whereas δ_D is proportional to a. If A/kT

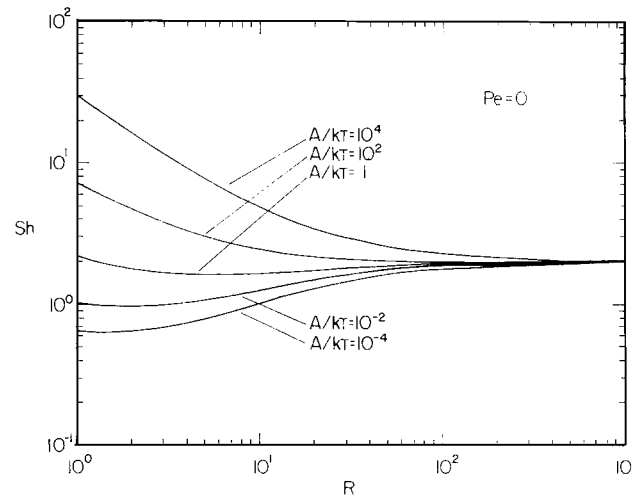

Fig. 5. Case 3. Sherwood numbers for the transport of finite size particles through a stagnant fluid to a spherical collector under the action of diffusion and London forces.

is small so that $\delta_F << \delta_m$, then as the aspect ratio R decreases at constant A/kT, δ_m becomes comparable to δ_D, and the variation in the diffusion coefficient begins to inhibit the transport. If A/kT is large so that $\delta_m << \delta_F$ then, decreasing R at constant A/kT, δ_F becomes comparable to δ_D and the transport rate is enhanced due to the action of the London forces.

Reported values of A/kT nearly always are in the range $10^{-2} < A/kT < 10^2$. Thus Figure 5 shows that, even in the best of circumstances ($R = 1$), this variation in Hamaker's constant by a factor of 10^4, results in a change in the Sherwood number by only a factor of 7. Particle transport rates in stagnant fluids are not highly sensitive to small changes in Hamaker's constant.

General Results

The results presented in Figure 6 do not contain any of the approximations which lead to the three special cases which have been discussed previously. They were obtained by solving the general transport Equation (8). Limiting behaviors can, however, be observed.

Dashed lines (- - -) represent the Levich-Lighthill equation (19). For Peclet numbers less than unity, the Sherwood numbers correspond to those computed for a stagnant fluid (Case 1c or Case 3) using Equation (26). At very large Peclet numbers the solid curves become tangent to the dotted lines (. . . . .) which represent the Sherwood numbers computed by neglecting Brownian motion (Case 2). The dotted curves were deduced from Figure 4, using Equation (14) to relate Sherwood number and capture efficiency, together with Equation (20) to relate Ad to A/kT and the Peclet number.

Criteria for Neglecting London forces or Brownian Motion

How small must the Peclet number be in order that $\delta_F << \delta_D$ for a given R and A/kT? How large must Peclet number be so that $\delta_D << \delta_F$ for the same R and A/kT? Answers to these questions are useful to design experiments that study London forces in the absence of Brownian motion or in analyzing a particular process to determine which effect is dominant.

Let the convective-diffusion-controlled region be defined as those sets of conditions (Pe, R, A/kT) for which the rate may be calculated to within 10% by ignoring London forces. Similarly, let the London-force-controlled region be those sets of conditions for which the rate may be calculated to within 10% by ignoring Brownian motion. These definitions suggest a method for determining limits for the regions.

In the convective-diffusion-controlled region, the rate should be independent of the value of A/kT. Selecting arbitrary values for the Peclet number and aspect ratio, the Sherwood number is first calculated for $A/kT = 0$. Then the value of the ratio A/kT is gradually increased,

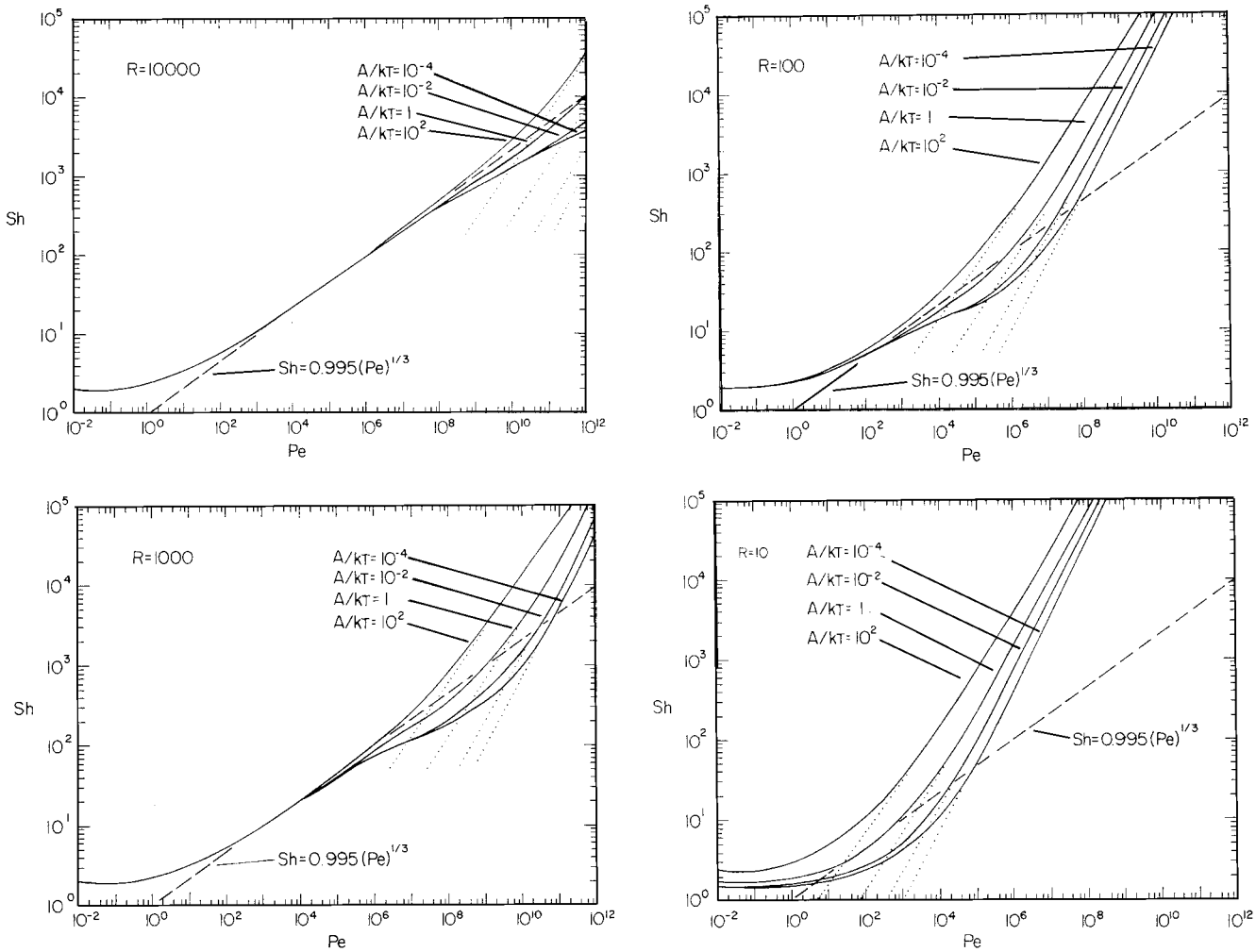

Fig. 6. Sherwood numbers computed for the transport of finite particles to a spherical collector under the combined action of convective-diffusion and London forces. Values of the aspect ratio are (a) $R = 10^4$, (b) $R = 10^3$, (c) $R = 10^2$, and (d) $R = 10$. For each aspect ratio, the value of A/kT was taken (upper curves to lower curves) as 10^2, 1, 10^{-2}, and 10^{-4}. Dashed lines represent the Levich-Lighthill equation (19), while the dotted curves represent Sherwood numbers deduced from Figure 4 which ignores the transport from diffusion.

holding Pe and R fixed, until the Sherwood number has increased to a value that is 1.1 times its initial value. In this manner one point (Pe, R, A/kT) on the boundary of the convective-diffusion region has been determined.

Within the London-force-controlled region the value of the collection efficiency depends only upon the values of R and the product $\frac{4}{3}\left(\frac{A}{kT}\right)\frac{R^3}{Pe}$ (denoted Ad). Arbitrarily selecting values for R and Ad, the efficiency is first computed for a value of the Peclet number that is sufficiently large so that no further change in the efficiency can be noted by changes in the Peclet number. Then the Peclet number and A/kT are gradually diminished, maintaining R and Ad fixed, until the efficiency increases by a factor of 1.1. In this manner one point on the boundary of the London-force controlled region is determined. Figure 7 summarizes the results. Selection of Pe/R^3 as the ordinate removes most of the R-dependence from the location of the boundaries.

Having established bounds on the regions where $\delta_F << \delta_D$ and $\delta_D << \delta_F$, it is now possible to summarize the conditions of validity for each of the limiting cases discussed. This summary is reported in Table 3 along with the corresponding rates of deposition.

Effect of Gravitational forces

Components of the gravitational force may be included in the radial and tangential force balances, given by Equations (3) and (4), to yield

$$\frac{v_r}{m} = \frac{s_r f_2}{m_\infty} - \frac{2}{3}\frac{Aa_p^3}{(h+2a_p)^2h^2} - \frac{4\pi}{3}a_p^3(\rho_p-\rho)\,g\cos\theta, \quad (27a)$$

and

$$v_\theta = s_\theta f_3 + \frac{4\pi}{3}a_p^3(\rho_p-\rho)\,g\sin\theta\,\frac{f_4(h/a_p)}{6\pi\mu a_p}, \quad (27b)$$

where $f_4(H)$ is the correction factor for the wall effect upon the tangential mobility. Goldman et al. (1967a) determined values for f_4 by considering the slow viscous motion of a sphere, through a quiescent fluid, parallel to a wall. A new dimensionless group—$G = \frac{4}{3}\pi a_p^4(\rho_p-\rho)g/kT$—appears upon nondimensionalization of Equation (27). This group may be interpreted as the ratio of the gravitational potential of a particle, located one particle radius from the collector, to the characteristic thermal energy.

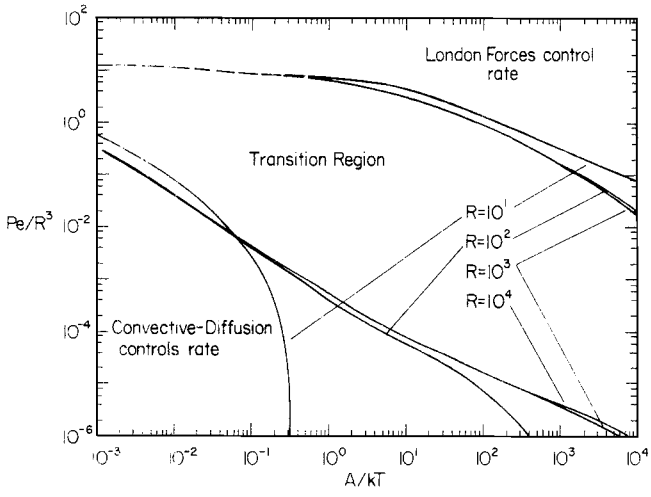

Fig. 7. Identification of regions in which either London forces or diffusion may be neglected when calculating the rate of deposition.

Table 3. Transport Rates and Regions of Validity for Limiting Cases

Case[a]	Region of validity[b]	Rate[b]
1a	$100 < Pe < \min[10^{-4}R^3, g_7(R, A/kT)]$	$Sh = 0.995\,(Pe)^{1/3}$
1b	$1 < Pe < \min[10^{-4}R^3, g_7(R, A/kT), 100]$	$Sh = g_3(Pe)$
1c	$Pe < \min[1, g_7(R, A/kT)]$ $R > 100$	$Sh = 2$
1d	$Pe < g_7(R, A/kT)$ $R > \max(Pe^{1/3}, 10)$	$Sh = g_3(Pe, R)$
2a	$g_7(R, Pe) < A/kT < 10^{-6}R^4Pe$	$eR^2 = g_4(Ad)$
2b	(see discussion)	$eR^2 = 1.5$
2c	$A/kT > g_7(R, Pe)$	$eR^2 = g_4(Ad, R)$
3	$Pe < 1$	$Sh = g_5(R, A/kT)$

[a] Refer to Table 2 for description of Cases.
[b] Value of the function $g_i(\ldots)$ may be evaluated from Figure i.

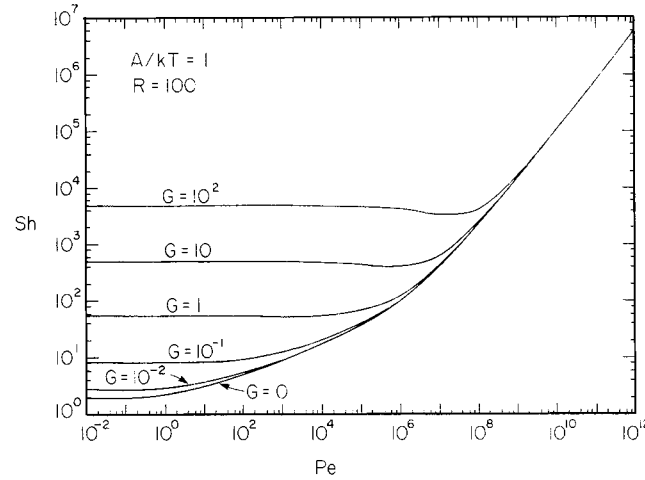

Fig. 8. Effect of gravitational forces upon the rate of deposition for a particular aspect ratio and Hamaker's constant.

Figure 8 shows the effect which gravitational forces have upon the deposition rates for one typical situation, namely $A/kT = 1$ and $R = 100$. In the extreme case in which gravitational forces completely dominate the process, one could expect the particles to travel at their terminal velocity v_z along straight, vertical trajectories which leads to deposition at a rate $I = \pi a^2 v_z c_z$. In dimensionless terms this result is expressed by

$$Sh = \frac{1}{2}RG \quad (28)$$

which agrees well with the results of Figure 8 at small Peclet numbers and $G > 1$.

As an example, 0.25-micron (radius) particles with a density of 1.1 g/cm³ correspond to $G \sim 0.01$. Particles of this radius or smaller are not influenced significantly by gravity, according to Figure 8. However, deposition of larger particles is affected by gravity at small Peclet numbers.

Adequacy of Additivity Rule

In lieu of giving rigorous consideration to the effects of coupling between transport mechanisms, as was done in

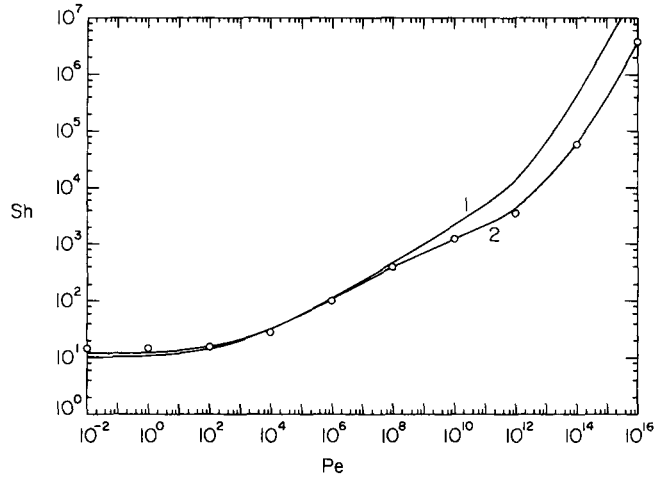

Fig. 9. Adequacy of the additivity rule for $R = 10^4$ and $A/kT = 10^4$. Lower curve represents results obtained by summing individual contributions from gravitational forces [Equation (28)], Brownian motion (Figure 3), and London forces (Figure 4). Points were obtained from simultaneously considering all effects, while upper curve is Eq. (29).

the present paper, the individual contributions to the deposition rate from each mechanism may be computed separately and subsequently summed to yield an approximation to the total deposition rate. This procedure, known as the additivity rule, was tested by Yao et al. (1971) and found to be adequate for practical calculations. Their transport equation, however, ignores the difference between non-Brownian particle velocity and fluid velocity as well as the variation of the diffusion coefficient with distance. It is of interest to retest the additivity rule after including the considerations ignored by them. Figure 9 compares the deposition rates computed by (1) a rigorous consideration of coupling effects, (2) summing individual contributions taken from Figures 3 and 4 together with Equation (28), and (3) the equation of Yao et al.:

$$Sh = \frac{1}{2} RG + 0.995(Pe)^{1/3} + \frac{3}{8}\frac{Pe}{R^2} \qquad (29)$$

For the conditions selected, three regions may be distinguished. Gravitational forces, Brownian motion, or London forces dominate for small, moderate, and large Peclet numbers, respectively. Agreement between (1) and (2) is quite good, whereas (1) and (3) differ by an order of magnitude at high Peclet numbers. This difference stems from the distinction between particle velocities and fluid velocities ignored in the analysis of Fuchs (1964) and Yao et al. (1971). However, if this distinction is considered in each of the individual contributions, the additivity rule yields results, in an easy manner, which agree reasonably well with the results obtained from a rigorous consideration of coupling effects.

NOTATION

a = radius of collector, cm
a_p = radius of particle, cm
A = Hamaker's constant, erg
$Ad = \frac{4}{3}\left(\frac{A}{kT}\right)\frac{R^3}{Pe}$
b, b_1, b_2, n = parameters in transformation of the radial variable
c = local concentration of particles, particles/cm^3
c_∞ = concentration of particles far from collector, particles/cm^3
$C = c/c_\infty$
D = local diffusion coefficient, cm^2/s
D_∞ = diffusion coefficient far from collector, cm^2/s
e = capture efficiency, $e = I/\pi a^2 \beta U c_\infty$
E = height of interaction energy barrier, erg
f_1, f_4 = correction factor for effect of wall proximity on radial and angular particle mobilities
f_2, f_3 = universal functions used to relate fluid and particle velocities
g_i = function whose value may be deduced from Figure i
G = $4/3\ \pi a_p^4(\rho_p - \rho)\ g/kT$
h = minimum separation between collector and particle surfaces, cm
h_{max} = separation at which ϕ is maximum, cm
h_{min} = separation at which ϕ is minimum, cm
H = h/a_p
I = rate of deposition, particles/s
k = Boltzmann's constant, erg/°K
m = mobility coefficient, cm/dyne-s
m_∞ = mobility coefficient far from collector, cm/dyne-s
N_r = radial particle flux, particles/cm^2-s
N_θ = angular particle flux, particles/cm^2-s
Pe = Peclet number, $Pe = 2a\beta U/D_\infty$
r = radial position of particle center, cm
R = aspect ratio, $R = a/a_p$
s_r = radial fluid velocity, cm/s
s_θ = angular fluid velocity, cm/s
Sh = Sherwood number, $Sh = 2I/4\pi a D_\infty c_\infty$
T = absolute temperature, °K
u = $v_\theta/\beta U$
U = approach velocity, cm/s
v = $v_r/\beta U$
v_r = radial particle velocity, cm/s
v_θ = angular particle velocity, cm/s
v_∞ = terminal velocity of particle far from collector, cm/s
Y = $H + 1$

Greek Letters

α = integration constant, particles/s
α_1, α_2 = proportionality constants
β = flow parameter
$\delta_D, \delta_F, \delta_m$ = characteristic lengths defined in Table 1, cm
η = transformed radial position
θ = angular position of particle center
μ = fluid viscosity, g/cm-s
ρ = fluid density, g/cm^3
ρ_p = particle density, g/cm^3
ϕ = total interaction energy, erg

LITERATURE CITED

Brenner, H., "The Slow Motion of a Sphere through a Viscous Fluid towards a Plane Surface," *Chem. Eng. Sci.*, **16**, 242 (1961).

Crank, J., and P. Nicolson, "A Practical Method for Numerical Evaluation of Partial Differential Equations of the Heat Conduction Type," *Proc. Camb. Phil. Soc.*, **43**, 50 (1947).

Fuchs, N. A., *The Mechanics of Aerosols*, MacMillan, New York (1964).

Goldman, A. J., R. G. Cox, and H. Brenner, "Slow Viscous Motion of a Sphere Parallel to a Plane Wall—I Motion through a Quiescent Fluid," *Chem. Eng. Sci.*, **22**, 637 (1967).

Goldman, A. J., R. G. Cox, and H. Brenner, "Slow Viscous Motion of a Sphere Parallel to a Plane Wall—II Couette Flow," *ibid.*, **22**, 653 (1967).

Goren, S. L., and M. E. O'Neill, "On the Hydrodynamic Resistance to a Particle of a Dilute Suspension when in the Neighborhood of a Large Obstacle," *ibid.*, **26**, 325 (1971).

Hamaker, H. C., "The London-van der Waals Attraction between Spherical Particles," *Physica*, **4**, 1058 (1937).

Happel, J., "Viscous Flow in Multiparticle Systems: Slow Motion of Fluids Relative to Beds of Spherical Particles," *AIChE J.*, **4**, 197 (1958).

Levich, V. G., *Physiocochemical Hydrodynamics*, Prentice-Hall, New Jersey (1962).
Lighthill, M. J., "Contributions to the Theory of Heat Transfer through a Laminar Boundary Layer," *Proc. Roy. Soc.*, **A202**, 359 (1950).
Ruckenstein, E., and D. C. Prieve, "Rate of Deposition of Brownian Particles under the Action of London and Double-Layer Forces," *J.C.S. Faraday II*, **69**, 1522 (1973).
Spielman, L. A., and J. A. Fitzpatrick, "Theory for Particle Collection under London and Gravity forces for Application to Water Filtration," *J. Colloid Interface Sci.*, **43**, 51 (1973).
Spielman, L. A., and S. K. Friedlander, "Role of the Electrical Double-Layer in Particle Deposition by Convective-Diffusion," *J. Colloid Interface Sci.*, **44**, 22 (1974).
Vrentas, J. S., J. L. Duda, and K. G. Bargeron, "Effect of Axial Diffusion of Vorticity on Flow Development in Circular Conduits: Part I. Numerical Solutions," *AIChE J.*, **12**, 837 (1966).
Yao, K. M., M. T. Habibian, and C. R. O'Melia, "Water and Waste-Water Filtration: Concepts and Applications," *Environ. Sci. Tech.*, **5**, 1105 (1971).
Yuge, T., "Theory of Heat Transfer of a Heated or Cool Body in High Speed Gas Flow," Rept. Inst. High Speed Mechanics of Tohoku Univ., **6**, 143 (1956).

Manuscript received May 29, 1974; revision received and accepted by September 16, 1974.

Distribution Coefficients at High Dilution for Organic Solutes Between Water and Isobutane or Isobutylene

To facilitate design of an extraction process for removal of organic solutes from petroleum and petrochemical waste streams, distribution-coefficient data were obtained for typical organic pollutants at high dilution. Volatile solvents were chosen because of their low solubility in water and because they are recovered easily. Samples from both the aqueous and the organic phase were analyzed chromatographically. To remove a sample from an equilibrium cell operating at pressures well above atmospheric, a special technique was developed using low-melting Indalloy for micro-encapsulation.

Distribution coefficients at ambient temperature are given for a variety of solutes, including esters, phenolics, ketones, and aldehydes. The results are correlated by a simple relation based on a perturbed-hard-sphere theory for dilute solutions. Isobutane or isobutylene may be particularly useful in a dual-solvent extraction process wherein a polar organic solvent is used to remove phenolics from water and the volatile C_4 hydrocarbon is used in a secondary extraction to remove the polar solvent from water.

K. W. WON
and
J. M. PRAUSNITZ
Chemical Engineering Department
University of California
Berkeley, California 94720

SCOPE

Extraction of organic solutes from industrial wastewaters provides one possible method for water-pollution abatement and for recovery of solutes having economic value. While extraction processes using conventional organic solvents have often been described, little attention has been given to the use of low-molecular weight hydrocarbon solvents for extraction from aqueous solutions. While an extraction process using volatile solvents must operate at elevated pressure, these solvents offer two important advantages: their solubility in water is extremely low and solvent recovery is simple.

While volatile hydrocarbons may, in some cases, efficiently remove organic pollutants from industrial wastewaters, their maximum utility may be in a dual-solvent extraction process applicable to aqueous waste streams containing phenolics and similar hard-to-remove organic pollutants. In such a process, the primary extraction uses a polar organic solvent of low volatility which effectively

K. W. Won is with Fluor Engineers and Constructors, Inc., Los Angeles, California 90040.